Title
Ovarian Teratomas in Women With Anti-N-methyl-D-Aspartate Receptor Encephalitis

Journal
The American Journal of Surgical Pathology, 43(7)

ISSN
0147-5185

Authors
Nolan, Amber
Buza, Natalia
Margeta, Marta
et al.

Publication Date
2019-07-01

DOI
10.1097/pas.0000000000001249

Peer reviewed

Ovarian Teratomas in Women with Anti- N-methyl-D-Aspartate Receptor Encephalitis: Topography and Composition of Immune Cell and Neuroglial Populations Is Compatible with an Auto-immune Mechanism of Disease

Amber Nolan MD PhD (1), Natalia Buza MD (2), Marta Margeta MD PhD* (1), Joseph T. Rabban MD MPH* (1)

(1) University of California San Francisco, Department of Pathology
(2) Yale University School of Medicine, Department of Pathology

*these authors contributed equally to the study.

Corresponding Author:

Joseph T Rabban MD MPH
UCSF Pathology Department
1825 4th Street, M-2359
San Francisco, CA 94158
joseph.rabban@ucsf.edu
office: 415-353-2292
fax: 415-353-1200

This work was presented in part at the 2014 Annual Meeting of the United States and Canadian Academy of Pathology and at the 2015 Annual Meeting of the American Association of Neuropathologists.

Funding Sources:

This work was supported by the USCF Department of Anatomic Pathology Resident Research Fund.

Financial Disclosures:

Dr Rabban reports the following:
-Commercial entity: Merck & Co.
-Disclosure: Spouse receives salary and stock options

Dr. Margeta reports the following:
-Commercial entity: Audentes Therapeutics
-Disclosure: Neuromuscular pathology consultant

Key Words: Teratoma, Anti-NMDAR Encephalitis, Inflammation, Neurons, Astrocytes

Short Running Title: Ovarian Teratoma in Auto-immune Encephalitis

ABSTRACT

Anti-N-methyl-D-aspartate receptor (NMDAR) encephalitis is an autoimmune syndrome in young women that is often accompanied by an ovarian teratoma (NMDAR-E teratoma). A prevailing theory implicates that the generation of auto-antibodies to NMDAR on neurons in the central nervous system is triggered by neuroglial tissue in the associated teratoma. The histopathology of NMDAR-E teratomas has not been fully elucidated but limited studies have focused on alterations in neuroglial tissues and immune cell populations. We hypothesized that evidence of antibody generation in NMDAR-E teratomas could be detected by co-localized neuroglial tissue and lymphoid aggregates with germinal centers as well as by alterations in the composition and morphology of neuroglial tissues. The study compared 12 NMDAR-E teratomas (11 ovarian, 1 mediastinal) to 61 control teratomas containing neuroglial tissue from women without NMDAR-E. NMDAR-E teratomas were significantly smaller and were composed of a higher percentage of neuroglial tissue than control teratomas. Many NMDAR-E teratomas did not exhibit typical gross pathologic features of a mature cystic teratoma, but were composed of predominately solid tissue (so-called Rokitansky nodule). Co-localized neuroglial tissue and lymphoid aggregates with germinal centers were present in 11/12 NMDAR-E teratomas, predominantly within the Rokitansky nodule, but only in 4/61 control teratomas ($p<0.0001$). There was a relative paucity of mature neurons in NMDAR-E teratomas as well as a hypercellular astrocyte population, while there were less prominent or no differences in the presence or composition of diffuse inflammatory infiltrates, lymphoid aggregates without germinal centers, ganglion cell clusters or oligodendrocytes between NMDAR-E teratomas and control teratomas. We conclude that the presence of co-localized neuroglial tissue and lymphoid aggregates with germinal centers along with a general paucity of neurons should prompt clinical consideration for NMDAR encephalitis even in asymptomatic women, since the symptoms may occasionally develop after an otherwise incidental oophorectomy. Tissue sampling should be directed to the Rokitansky nodule, when present, to identify neuroglial tissues; complete microscopic examination of the ovarian specimen should be considered if gross pathologic features of teratoma are not present.

The significance of the altered neuroglial cell populations and potential relationship to the pathogenesis of NMDAR encephalitis merit further study.

INTRODUCTION

Anti-N-methyl-D-Aspartate receptor (NMDAR) encephalitis is an autoimmune syndrome defined by the presence of antibodies to NMDA receptor, a neuronal cell-surface ligand-gated cation channel involved in glutamatergic synaptic transmission. Neurologic symptoms often initially manifest as confusion, agitation and personality changes but then rapidly progress to psychosis, dyskinesia, seizures, autonomic instability and respiratory collapse.[1, 2] The syndrome predominantly affects young women and is often designated as a paraneoplastic syndrome because an ovarian teratoma has been detected in about half of affected women; rare cases of primary extra-gonadal teratoma or carcinoma have also been described in this syndrome.[3] Nearly all of these tumors contain a component of mature or immature neuroglial tissue, a finding that is slightly less common in control ovarian teratomas in women without encephalitis. Reduction of the anti-NMDAR antibody titer following immunotherapy and surgical removal of the ovarian tumor, if present, is associated with clinical improvement in most patients.[2, 4]

Based on these observations, a paraneoplastic mechanism of disease has been proposed: disruption of immunologic self-tolerance to NMDAR expressed by neuroglial tissue in the ovarian teratoma results in abnormal production and circulation of NMDAR antibodies that subsequently enter the CNS, leading to encephalitis.[5, 6] The mechanism for a break in immune tolerance is unclear but triggering events such as viral infection or genetic predisposition have been proposed [7, 8]. A paraneoplastic mechanism of disease may not explain all cases of this syndrome, since some patients do not have a detectable tumor. In those that do, however, it is conceivable that morphologic manifestations of a paraneoplastic process might be visible in routine microscopic examination of the tumor itself; specifically, altered immune cell populations and altered neuroglial elements. Few studies have evaluated the histopathology of NMDAR encephalitis-associated (NMDAR-E) teratomas.[2, 7-13] The topography and composition of immune cell populations in these tumors (B lymphocyte-rich infiltrates and lymphoid aggregates with germinal centers localized in and around neuroglial elements) and the demonstration of NMDAR expression within the neuroglial elements have been reported as evidence in keeping with an auto-immune model of

pathogenesis. Altered morphology of the neuroglial elements has been described as further support of this model. However, the literature is limited by the scant number of studies, by small sample sizes and by differing study designs, making it challenging to compare results and leading to some conflicting observations, particularly in comparison to control teratomas.

The aim of the current study was to determine whether the morphologic, immunophenotypic, and topographic properties of the immune cell populations and the neuroglial populations distinguish NMDAR-E teratomas from ovarian teratomas containing mature neuroglial elements in women without NMDAR-E (herein referred to as control teratomas). As described by others in smaller series, we hypothesized that the presence and topography of B-cell infiltrates and lymphoid aggregates with germinal centers in and around neuroglial elements would distinguish the NMDAR encephalitis-associated ovarian teratomas (NMDAR-E teratomas) from control teratomas. We also hypothesized that the neuroglial and ganglion cell populations in NMDAR teratomas would exhibit alterations in cell number, distribution, and/or morphologic and immunophenotypic properties compared to control teratomas. In addition to the potential implications for understanding pathogenesis of this syndrome, awareness of the gross pathologic and morphologic hallmarks of NMDAR teratomas is valuable to diagnostic pathologists because in a minority of instances the neurological manifestations of the syndrome develop after an otherwise incidental ovarian teratoma is removed.[10, 14]

MATERIALS AND METHODS

Case and control selection

With approval from our institutional review boards, 12 women with NMDAR encephalitis who had a concurrent teratoma of the ovary (n=11) or mediastinum (n=1) surgically resected were identified from our pathology archives. Ten women underwent surgery at University of California San Francisco (UCSF), San Francisco, CA and 2 women

underwent surgery at Yale-New Haven Hospital, New Haven, CT. The criteria for the diagnosis of NMDAR encephalitis were based on the clinical evaluation by the treating neurologist as documented in the electronic medical record and based on the presence of stereotypical symptoms and progression over time. The clinical diagnosis was confirmed by a positive test result for NMDAR antibody titer in the serum and/or cerebrospinal fluid in 10 of 10 women who were tested (NMDAR antibody titers were not tested in the remaining 2 women). The time interval between clinical diagnosis and oophorectomy was recorded as was the pre-operative use of immunosuppressive therapy.

A control group was formed of women without encephalitis who had an ovarian mature teratoma containing neuroglial tissue (so-called control teratoma) removed at UCSF. The electronic medical records were reviewed to confirm that none of these patients with control ovarian teratoma had concurrent encephalitis. To establish a case-control ratio of 1 to 5, a total of 61 women were included in the control group after microscopic examination of consecutive specimens from our pathology archives. Ovarian teratomas lacking any neuroglial tissues were excluded as were tumors that contained any component of malignancy. The control group was also selected to roughly match the age distribution of the NMDAR-teratomas. Thus, about 20% of the cases and of the controls were under 18 years old.

Gross pathologic evaluation

The size (maximum diameter) of each teratoma was obtained from the pathology report gross description; if a tumor was received in fragments, the size described in the pre-operative radiology report was used. Gross specimen photographs were available for most of the cases to supplement the findings in the gross description. Cysts were classified as simple if they were unilocular, had a smooth inner lining, and were devoid of any clear features of teratoma such as hair, sebum, bone and/or cartilage. Otherwise, the presence of these grossly visible findings in the cysts was reported as consistent with a teratoma. The presence or absence of a solid fibrofatty nodule

emanating from the inner cyst lining (so-called Rokitansky nodule [15]) was recorded; if present, the size of the nodule relative to the size of the cyst was also recorded.

Lymphoid tissue evaluation

The lymphoid populations were evaluated within and adjacent to neuroglial tissues (both CNS-like neuropil and ganglion cell clusters) as well as in areas of non-neural tissue and were classified as lymphoid infiltrates, lymphoid aggregates with germinal centers, and lymphoid aggregates without germinal centers. Lymphoid infiltrates, when present, were subjectively classified as low-cellularity versus high-cellularity diffuse infiltrates. The lymphoid density was also quantified by counting the number of lymphocytes per 400X total magnification high power fields (hpf) in the areas of highest density in the routine hematoxylin and eosin (H&E) stained slides. In selected tumors with a high lymphoid density, cell counts per hpf were also conducted using immunohistochemically stained slides with the following antibodies: CD20, CD3, CD138, and FOXP3 (a marker of both natural T regulatory cells (nTregs) and adaptive / induced T regulatory cells (a / iTregs)). In addition, the number of lymphoid aggregates was determined by counting all lymphoid aggregates (arbitrarily defined as clusters of 50 or more lymphocytes) adjacent to neuroglial or non-neural tissues; lymphoid aggregates with germinal centers were identified based on the presence of large cells in the center of the aggregate.

Neuroglial tissue evaluation

Neuroglial tissue was categorized into two populations: a.) central nervous system (CNS) - like neuropil usually containing neurons (cells with large nuclei, open chromatin, prominent nucleoli, and variable Nissl substance), astrocytes (cells with indistinct cytoplasm and oblong nuclei with granular chromatin), and oligodendrocytes or b.) ganglion cell clusters (large neurons resembling dorsal root ganglia, surrounded by satellite cells) not associated with neuropil. The amount of all neuroglial tissues in each teratoma was approximated by calculating the percentage of the total surface area of tumor in each slide occupied by neuroglial tissue. The number of tissue sections

containing neuroglial tissue was recorded. A tissue section was defined as a single specimen slice; in most cases each glass slide contained a single tissue section, but some contained more than two or more tissue sections.

The density of individual cell types per high power field within neuroglial tissue was calculated on routine H&E stained slides. In selected cases and controls with the highest lymphoid density, the cell counts were also performed on immunohistochemically stained slides using the following antibodies: NeuN (a marker of mature neurons), MAP2 (a marker of mature neurons, glial precursor cells, and some neoplastic glial cells) and OLIG2 (a marker of oligodendrocytes).

Immunohistochemical methods

Staining for NeuN (A60, Chemicon, 1:4000), MAP2 (microtubule-associated protein 2, HM2, Sigma, 1:20,000), CD20 (MJ1, Leica, prediluted), CD3 (LN10, Leica, prediluted), and CD138 (MI15, Leica, prediluted) was performed in our clinical laboratory on the Leica BOND III automated immunohistochemistry platform using a range of epitope retrieval incubation times (from 0-30 minutes). Staining for FOXP3 (1:50, ABCAM20034), was performed on the Ventana Benchmark XT platform in the UCSF Brain Tumor SPORE Tissue Core (NIH/NCI P50 CA097257). Unstained slides for the FOXP3 staining were deparaffinized, unmasked with a Tris-based buffer at a pH of 8.5 for 30 minutes, exposed to hydrogen peroxide for 8 minutes, incubated with the primary anti-FOXP3 antibody for one hour, then visualized with secondary immunoreagents and DAB substrate and counterstained.

Statistics

All data were analyzed with GraphPad Prism 7 statistical software. For evaluating normality, both the D'agostina-Pearson omnibus and the Shapiro-Wilk tests were used. To be considered non-parametric, the distribution had to exhibit an alpha <0.01 for both tests. Difference in variance was determined using an F test. Statistical significance

between groups was determined using a two-tailed *t*-test if the data was normally distributed. If there was a significant difference in variance between groups, Welch's correction was added to the two-tailed *t*-test. If data were non-parametric, a Mann-Whitney U test was used. A Fischer's exact test was used to analyze the proportion of cases with and without a specific pathology. Statistical significance was defined as $p<0.05$.

RESULTS

Clinical presentation

The average age of the 12 women with an NMDAR-E teratoma was 25 years (range, 13 to 36 years); two of the 12 (20%) were younger than 18. By design, the women in the control group had a similar age distribution (average age 26 years, range 4 to 48). The symptoms developed over the course of weeks to months, initially presenting with prodomal fever and/or persistent headache (5/12 women), followed by abrupt onset of erratic mood, speech and behavior (10/12) and visual/auditory hallucinations (6/12). These symptoms eventually progressed to seizures and respiratory failure requiring mechanical ventilation in 10 of 12 women; 9 of these 10 women initially presented to another hospital where they were first managed in an intensive care unit environment for a median of 22.5 days (range 5 to 72 days) before transfer to one of our hospitals. Seven of these 9 women were intubated during the initial hospitalization, including 4 of whom had prolonged ventilator-dependency leading to tracheostomy prior to transfer. The diagnosis of autoimmune encephalitis was pursued at the original hospital in 4/9 women; for the remainder, the diagnostic considerations included infectious meningitis, central nervous system lymphoma, seizure disorder, and/or schizophrenia. Two of the 12 women initially presented directly to our hospital with altered mental status and bizarre behavior but without seizures or respiratory failure.

At the time of presentation at our hospitals, NMDAR encephalitis was considered as a possibility in each patient and pelvic imaging was performed to evaluate for ovarian

teratoma. Radiologic evidence of an ovarian cyst or mass was present in 9/11 women whereas a mediastinal mass consistent with teratoma was identified in 1 woman, whose ovaries were radiologically normal. The median time interval from radiologic detection of the teratoma to surgery was 1.5 days for the 9 women with an ovarian teratoma; the woman with a mediastinal teratoma presented with symptoms limited to memory loss and mild mood alterations, and her surgery occurred 24 days after radiologic detection. Pre-operative immunosuppressive therapy (steroids, plasmapheresis, Rituximab, and/or intravenous immunoglobulin) was administered in 10/12 women without significant immediate effect on neurologic status pre-operatively.

The surgical procedures were unilateral oophorectomy with or without salpingectomy (10 women), unilateral ovarian cystectomy (1 woman), and mediastinal tumor resection (1 woman). Intraoperatively, the ovary appeared cystic (7 women) or normal (3 women); the intraoperative appearance of the ovary was not reported for 1 woman. In the 1 woman with a mediastinal teratoma, the tumor arose in the left anterior mediastinum.

Post-operatively, only 1 of the women requiring pre-operative mechanical ventilation improved to the point of extubation within a few days after surgery. Most of the rest experienced slowly improving but persistent autonomic storming and remained ventilator-dependent at the time of transfer to a rehabilitation hospital at a median of 27 days (range 3 to 180 days) after surgery; one patient died of toxic megacolon 83 days after surgery. Median post-discharge follow up time was 33 months (range 2.4 to 88 months). One woman required continued hospitalization. The remainder regained autonomic stability, although only one woman returned to her baseline cognitive function and the majority continued to experience mild to moderate degrees of residual neurologic impairment.

Gross pathology

The clinical diagnosis of NMDAR encephalitis was communicated to the pathologist at the time the surgeon submitted the specimen for pathologic evaluation in 10/12 women. In the remaining two women, the submitted clinical history was chronic respiratory failure in one woman and a symptomatic ovarian follicular cyst in the other woman.

The ovarian teratoma was unilateral in all 11 women; in contrast, 20% (12/61) of the women in the control group had bilateral ovarian teratomas. The specimen was an intact ovary containing cysts in 9/11 women whereas in the other two women the specimen consisted of multiple fragments of cyst in wall (Figs. 1-3). In 7/11 specimens, the teratoma was predominantly composed of a Rokitansky nodule that nearly completely filled the cyst, leaving only a compressed rim of space containing sebaceous material around the nodule. For this reason, these 7 tumors grossly appeared more solid than cystic, although most of these specimens also contained multiple simple cysts in the ovarian parenchyma adjacent to the teratoma (these corresponded to follicle cysts on microscopic examination). Hair emanating from the surface of this nodule was present in 5/7 specimens, two of which also contained cartilage or bone. Among the 4 specimens without a Rokitansky nodule, the specimen consisted of fragmented cyst walls with matted hair and sebum in 1 woman. In the remaining 3 women, the specimen was an intact ovary containing multiple simple, smooth lined cysts without any hair, sebum, cartilage or bone to suggest a teratoma. Among the control teratomas, 22/61 consisted of an intact cyst and the remainder were fragmented. A Rokitansky nodule was present in 49/61 control teratomas. Nearly all of the control teratomas contained hair and sebaceous material while half contained bone or cartilage.

The median size of the NMDAR-E teratomas was 1.7 cm (range 0.7 to 5 cm), which was significantly smaller than that of the control teratomas (Table 1). The specimens were entirely examined microscopically in 9/12 women; representative sampling for microscopic examination was performed in 3/12 women. On average 8 cassettes of tissue were examined microscopically (range 3 to 15 cassettes). Paratubal cysts were visible in the fallopian tube of 4 of the 6 women who also underwent salpingectomy.

In the woman with a mediastinal teratoma, the specimen consisted of a 4.1 cm intact multicystic mass containing cartilage but no hair or sebaceous material (Fig. 3B).

Microscopic pathology

All 12 NMDAR-E teratomas contained neuroglial tissue as well as non-neuroglial tissues, the most common being keratinizing squamous epithelium, sub-cutaneous adnexal structures and adipose tissue, mucinous epithelium, and various mesenchymal tissues. In 11/12 NMDAR-E teratomas the neuroglial tissues were mature and in 1 tumor there was also a single microscopic focus of immature neural elements; in the latter case, the scant size did not meet criteria for classification as an immature teratoma.[16] The neuroglial tissues comprised only a small area of each tumor (Table 1); however, the neuroglial tissue represented a larger percentage of the total tumor in the NMDAR-E teratomas compared to the control teratomas (Table 1, Supplementary Fig.S1). Neuroglial tissue was not present in the frozen section samples of the two NMDAR-E teratomas that were evaluated intraoperatively.

There were two patterns of distribution of the neuropil-associated neuroglial tissue in the NMDAR-E teratomas. The first pattern, which was present in all 12 tumors, was a unifocal or multifocal solid irregularly shaped area of neuropil embedded within the center of the adipose tissue of the Rokitansky nodule (Fig. 4). In some cases, the neuropil was surrounded by small foci of bone, cartilage, and/or mucinous glandular elements. The second pattern (Fig. 5), which was present in 4/12 NMDAR-E teratomas, consisted of thin subependymal bands of neuropil along the wall of a cyst, recapitulating a ventricle of the central nervous system (also referred to as a glial cyst in older literature[15]). Ependyma lined the cyst walls. Tubulo-glandular ependymal structures were also embedded within the solid pattern component of neuropil in 4/12 NMDAR-E teratomas.

Compared to control teratomas, neuropil-associated neuroglial tissue in the NMDAR-E teratomas contained a paucity of mature neurons and a hypercellular population of

astrocytes. Whereas control teratomas contained 7 mature pyramidal neurons per high power field of neuropil, only 1 mature neuron per high power field of neuropil was present in NMDAR-E teratomas (Table 1, Fig. 6). In addition, these few remaining neurons often exhibited degenerative changes, such as shrunken or smudged nuclear contours, vacuolation of the cytoplasm, and variable chromatolysis (Fig. 6A-B). The relative absence of mature neurons in NMDAR-E teratomas was confirmed by NeuN immunohistochemistry (Table 1, Fig. 7A, D, G). Although the overall density of MAP2-positive cells was similar in NMDAR-E teratomas and control teratomas (Fig. 7H), there was no significant subpopulation of MAP2-positive (MAP2+) cells that correlated to the morphology of mature pyramidal neurons in NMDAR-E teratomas. In control teratomas, MAP2 immunohistochemistry typically labeled the cytoplasm of mature neuron-like cells with a granular background of staining in dendritic processes (Fig. 7B). In the NMDAR-E cases, on the other hand, MAP2 labeled the cytoplasm of small cells with stubby processes, with only focal granular background staining present (Fig. 7E); these cells were visible on the MAP2-stained slides, but their correlate was not apparent on the H&E stained slides.

Astrocytes were present at a higher density in NMDAR-E teratomas (Table 1, Fig. 8) and they also often exhibited striking dysmorphic alterations ranging from nuclei with hyperchromasia, enlargement and irregular contours, to large multinucleated cells with abundant gemistocytic cytoplasm or cells filled with abundant eosinophilic deposits. Reactive changes (including variable Rosenthal fibers and gemistocytic morphologies) were occasionally also observed in control teratomas. Oligodendrocytes were present to the same extent in NMDAR-E teratomas and control teratomas, as evaluated using OLIG2 immunohistochemistry (Fig. 7C, F, I).

Ganglion cell clusters were present in 5/12 (42%) of NMDAR-E teratomas but only in 10/61 (16%) of control teratomas (Table 1, Fig. 9). The total number of ganglion cell clusters ranged from 0 to 9 in the NMDAR-E teratomas and 0 to 7 in the control teratomas (Fig. 9E). None of the ganglion cell clusters were embedded within neuropil,

but in rare instances they were located in immediate proximity. None exhibited striking nuclear atypia or degenerative changes.

Diffuse lymphoplasmacytic infiltrates were present within neuropil-associated neuroglial tissue in 4/12 (25%) of NMDAR-E teratomas and in 26/61(43%) of control teratomas (Table 1, Supplementary Fig. S2). The ganglion cell clusters were rarely involved by these infiltrates in either type of teratoma. The overall lymphocyte density in neuroglial tissue was only slightly increased in NMDAR-E teratomas compared to control teratomas on routine H&E stained slides (Table 1, Supplementary Fig. S2); there was no difference in the density of B-cells, plasma cells, T-cells, or regulatory T-cells using immunohistochemistry (Table 1, Supplementary Fig. S2).

Lymphoid aggregates without germinal centers were present adjacent to neuropil-associated neuroglial tissue in all 12 NMDAR-E teratomas and were present adjacent to ganglion cell clusters in 4/5 (80%) NMDAR-E teratomas containing ganglion cell clusters (Table 1). The median number of lymphoid aggregates without germinal centers near neuroglial tissue was 3 per tumor. In contrast, lymphoid aggregates without germinal centers were present near neuropil-associated neuroglial tissue in 43/61 (70%) control teratomas and the median number of aggregates was 1 per tumor (Fig. 4H). Among the 9 control teratomas with ganglion cell clusters, adjacent lymphoid aggregates without germinal centers were only present in 1 tumor (Fig. 9G).

Lymphoid aggregates with germinal centers were more strongly associated with NMDAR-E teratomas. These were present surrounding neuropil-associated neuroglial tissue in 11/12 (92%) NMDAR-E teratomas but only in 4/61 (7%) control teratomas. In the NMDAR-E teratomas, the median number of these lymphoid aggregates with germinal centers was 3 per tumor, ranging from 0 in one tumor up to 7 in total in another tumor, while the median number of lymphoid aggregates with germinal centers was 0 in control teratomas (Fig. 4G). Among the 5 NMDAR-E teratomas containing ganglion cell clusters, only 2 exhibited adjacent lymphoid aggregates with germinal centers; none were found in the 9 control teratomas with ganglion cell clusters (Fig. 9F).

Non-neural teratomatous tissue (e.g. keratinizing squamous epithelium, cutaneous adnexal structures, mucinous glandular elements) was involved by diffuse lymphoplasmacytic infiltrates in 1/12 (8%) NMDAR-E teratomas and in 11/61 (18%) control teratomas (Table 1, Supplementary Fig. S3). Lymphoid aggregates without germinal centers involving non-neuroglial tissue were present in 11/12 NMDAR-E teratomas and in all 61 control teratomas. Lymphoid aggregates with germinal centers were present adjacent to non-neuroglial tissue in 5/12 (42%) NMDAR-E teratomas and in 15/61 (25%) control teratomas. Lymphoid aggregates without germinal centers were actually higher in control teratomas, likely due to the greater amount of non-neural tissue in these teratomas.

Non-teratomatous pathology

The non-neoplastic ovarian cortex adjacent to the NDMAR-E teratoma exhibited the expected appearance for a premenopausal ovary: oocytes in primordial, primary and secondary follicles; corpus luteum and corpus albicans (Supplementary Fig. S4). Multiple follicle cysts were present in 7/11 ovary specimens and epithelial inclusion glands or cysts were present in 4/11. A mucinous cystadenoma associated with intestinal-type teratomatous elements was present in 1 of the NMDAR-E teratoma specimens. There were no inflammatory infiltrates or lymphoid aggregates in the ovarian parenchyma or involving the fallopian tubes. Paratubal cysts were present in 4/6 salpingectomy specimens.

DISCUSSION

This study of 11 ovarian teratomas and 1 mediastinal teratoma in women with NMDAR encephalitis demonstrates alterations in the immune cell and neuroglial populations that are not present in control teratomas and therefore further substantiate the paradigm of a paraneoplastic mechanism for the encephalitis. Specifically, NMDAR-E teratomas were characterized by 1.) the presence of lymphoid aggregates with germinal centers around neuroglial tissue; 2.) the near absence of mature neurons within neuropil; and 3.) the

presence of hypercellular astrocyte populations. These observations carry practical implications for the pathologic evaluation of ovarian teratoma specimens as well as implications for understanding the mechanism of this syndrome.

Although more than five hundred cases have been reported since the syndrome of NMDAR encephalitis associated with ovarian teratoma was first described in 2005,[2, 3] there is scant literature on the histopathology of the ovarian teratomas in these patients; only 51 cases, excluding the current study, have been described in terms of the immune cell and/or neuroglial populations (Table 2).[2, 7-13] The prevailing theory for pathogenesis is that antibody-mediated injury to neurons in the hippocampus and prefrontal cortex of the brain is caused by auto-antibodies generated against NMDAR on the teratoma that cross the blood brain barrier [5, 6]; a causal relationship is suggested by the clinical observation that tumor resection is often followed by reduction of auto-antibody titers and clinical improvement.[2] This theory does not fully explain all cases as only about half of patients have a detectable tumor. The trigger for generation of auto-antibodies is not understood; viral infection has been proposed as one possible mechanism.[5] Nor is the mechanism by which the auto-antibodies cross the blood-brain barrier understood. Regardless of the initiating event, antibodies to NMDAR can be detected in the serum and/or cerebrospinal fluid of these patients.[3] Neuroglial tissues in the associated ovarian teratomas have been shown to express the two subunits of the NMDAR, NR1 and NR2.[2, 7, 9, 12] NMDAR have also been detected within germinal centers of lymphoid aggregates in an ovarian teratoma from the patient with this syndrome.[8] Autopsy brain findings from patients with NMDAR encephalitis are notable for regional loss of pyramidal neurons, neuronal degeneration, gliosis, and deposition of immunoglobulin in the hippocampus, basal forebrain, basal ganglia and spinal cord.[12] Therefore, a parallel constellation of alterations in the neuroglial and immune cell populations might be expected in the associated ovarian teratomas.

In our study, the density of mature neurons was strikingly reduced in NMDAR-E teratomas versus control teratomas whether evaluated by routine H&E staining or by NeuN staining. The cause of the relative absence of mature neurons in the NMDAR-E

teratomas is not clear; one potential explanation is that this represents the end stage result of sustained autoimmune injury to the neurons. In that case, a spectrum of damage ranging from varying degrees of degenerative changes to cell loss might be expected. One study has described degenerative changes in the neurons of two NMDAR-E teratomas [10], and indeed the few remaining neurons identified in this study often demonstrated shrunken or smudged nuclear contours, vacuolation of the cytoplasm, and variable chromatolysis. The increased density of astrocytes along with the dysmorphic/reactive features observed in this study could also reflect a prominent response to neuronal injury.

A response to neuronal injury might also explain the small cells with stubby processes that exhibit a MAP2+ / NeuN-negative (NeuN-) immunophenotype in the NMDAR-E teratomas. While mature neurons exhibit well-formed dendrites and a dual MAP2+, NeuN+ immunophenotype, these small cells with stubby processes may represent injured, degenerating neurons, in keeping with the autoimmune paradigm for this syndrome. In support of this interpretation, a similar loss of a NeuN+ immunophenotype has been described following neuronal injury in studies of axotomy and excitotoxicity.[17, 18] A second possibility comes from the observation that some neoplastic astrocytes can exhibit a similar morphology and immunophenotype, though it is unclear how such cells would fit into an autoimmune paradigm.[19] Dysplastic neuronal alterations similar to gangliogliomas have been described in a study of 4 NDMAR teratomas.[11] The criteria for defining dysplastic alteration were multinucleation, dysmorphic cell shape, and a clustered distribution of neurons; none of these features were definitively observed in the current study nor did any of the neuroglial tissue resemble a neuronal or glioneuronal neoplasm. We did however note occasional striking dysmorphic features in the astrocyte population including multinucleation. A third possibility comes from the observation that some glial and neuronal precursors exhibit the morphology of small cells with stubby processes and MAP2+, NeuN- immunophenotype.[19] Therefore, if MAP2+, NeuN- cell population in NMDAR-E teratomas represents a type of immature cell unique to this tumor syndrome, then it is conceivable that antigens on those cells could be responsible for triggering the

abnormal immune response to NMDAR. Of note, immature teratomas comprise up to 26% of the teratomas associated with NMDAR encephalitis, although none were observed in the current study.[1] Oncofetal antigens expressed by a variety of neoplasms are known to induce strong immune responses.[20] In particular, many paraneoplastic syndromes are associated with embryonal antigens expressed by pulmonary small cell carcinoma.[21] The nature of this distinct population of MAP2 positive / NeuN negative small cells merits further study, particularly with respect to its potential role in pathogenesis of this syndrome.

Similarly, the hypercellular astrocyte populations observed in the NDMAR-E teratomas but not in the control teratomas deserves further investigation. One study reported an abnormal glial population in 2 NMDAR-E teratomas, characterized by hypercellularity and, in 1 of 2 tumors, elevated proliferative activity measured by Ki-67 immunohistochemistry.[11] Whether the MAP2+, NeuN- small cells in the current study correlate with the abnormal glial population described by others is difficult to address because the earlier study did not evaluate MAP2 or NeuN staining.

Regarding the immune cell populations in NMDAR-E teratomas, our study validates the prior observation that co-localization of neuroglial tissue and lymphoid aggregates with germinal centers is a distinct feature that is not commonly present in control teratomas.[10] As reported for 3 of 5 NMDAR-E teratomas in that study, all but one NMDAR-E teratoma in the current study exhibited numerous lymphoid aggregates with germinal centers adjacent to neuropil-associated neuroglial tissue. Although similar findings were seen in a minority of control teratomas, the total number of lymphoid aggregates with germinal centers per tumor was significantly higher in the NMDAR-E teratomas. A recent study demonstrated that antibodies to the NMDAR subunits NR1 and NR2 can be detected within the germinal centers of such lymphoid aggregates; this suggests that the lymphoid aggregates neighboring the neuroglial tissues may be responsible for generating the auto-antibodies to NMDAR.

None of the other immune cell populations, such as diffuse infiltrates involving neuroglial tissue, specific subsets of immune cells (T-cells, regulatory T cells, B cells or plasma cells), or lymphoid aggregates without germinal centers, were as significantly associated with NMDAR-E teratomas in this study. Three studies reported increased immune cell populations (specifically B-cell populations in two of the three studies) involving neuroglial tissue in NMDAR-E teratomas compared to control teratomas.[7, 11, 12] Most of the patients in the current study were treated with immunosuppressive therapy prior to oophorectomy. It is possible that this may have diminished the immune cell populations in the NMDAR-E teratomas just enough such that any natural difference compared to control teratomas was not detectable; nevertheless, the presence of lymphoid aggregates with germinal centers remained a striking difference between the two teratoma types.

The practical implications of this study are two-fold. First, NMDAR-E teratomas may not exhibit significant ovarian enlargement or cystic features when viewed intraoperatively or grossly prior to dissection; the size of the tumor may be under 1 cm and on average is just under 2 cm. The small size is most likely due to the fact that these tumors were, by definition, asymptomatic in terms of the typical presentation of an ovarian cyst. Instead, these clinically occult tumors were detected only by radiologic screening as part of the work-up and management of NMDAR encephalitis. Even after specimen dissection, the cysts of NMDAR-E teratomas may occasionally be simple in gross appearance, without any specific features to suggest teratoma such as hair, sebum, cartilage or bone. Furthermore, large follicle cysts, occasionally the same size as the cystic teratoma, were also present in the majority of specimens in this study. Therefore, if the clinical history is suggestive of NMDAR encephalitis, the ovarian specimen should be thinly sliced in its entirety to look for evidence of any teratoma. If the gross findings are equivocal for evidence of a teratoma, complete submission of the entire ovary for microscopic examination is advised. Complete submission of the entire ovary should be considered even if there is gross evidence of teratoma, because the presence of neuroglial tissue may be limited to only one or two tissue sections of the entire specimen. In our study, the neuroglial tissues were most often embedded in adipose

tissue in the center of the Rokitansky nodule, as has been recognized by others as long as a century ago.[22-24] Therefore, at a minimum, tissue sampling should focused on the Rokitansky nodule. In a minority of cases in our study, neuroglial tissue was also present in a subependymal band-like distribution in cystic structures recapitulating ventricles. This has also been described by others and sometimes referred to as a glial cyst.[15, 23, 24] In our study, lymphoid aggregates with germinal centers was present in these areas as well. Thus, cyst-like areas also merit microscopic attention for possible neuroglial tissues. Finally, if the microscopic findings of a representatively-sampled ovary from a woman with suspected NMDAR encephalitis confirm a diagnosis of teratoma but neuroglial tissues are not identified, submission of the remaining tissue for microscopic examination is advised in an attempt to identify neuroglial tissue and evaluate for the presence of nearby lymphoid aggregates with germinal centers. Though this may not necessarily be essential to clinical care, documenting such findings is important for clinicopathologic correlation, particularly if the results of NMDAR antibody titers are still pending.

The second practical implication is that in the pathologic reporting of any ovarian teratoma, it may be of clinical value to document the presence of co-localized neuroglial tissue and lymphoid aggregates with germinal centers, even if there is no history of NMDAR encephalitis. At least two patients with NMDAR encephalitis have been reported to develop the onset of symptoms at a time point after an otherwise incidental removal of an ovarian teratoma.[10, 14] Therefore, alerting the clinician to the presence of this finding may be valuable to prompt immediate clinical correlation with the patient's neurological status and to prompt consideration of this syndrome if the patient develop prodromal symptoms at a later time. Because the early symptoms of NMDAR encephalitis are not specific, there is a broad differential diagnosis to consider; in fact, as reported in the literature and in our study, NMDAR encephalitis is often not among the leading clinical considerations, particularly in patients who are first managed by providers other than neurologists or mental health providers.[3] Early diagnosis of the syndrome before progression to severe symptoms and early intervention with immunotherapy are associated with a more favorable outcome.[3] By documenting the

presence of this relatively distinct morphology, the pathologist has an opportunity to contribute to early intervention in the, albeit rare, setting of post-oophorectomy onset of NMDAR encephalitis.

In summary, NMDAR-E teratomas are characterized by co-localization of neuroglial tissue and lymphoid aggregates with germinal centers, a finding that is uncommon in control teratomas. These tumors exhibit a relative paucity of mature neurons and a hypercellular astrocyte population. How these alterations in neuroglial cell populations are related to the pathogenesis of NMDAR encephalitis merits further study.

REFERENCES

1. Dalmau J, Gleichman AJ, Hughes EG, et al. Anti-NMDA-receptor encephalitis: case series and analysis of the effects of antibodies. *Lancet Neurol.* 2008;7:1091-1098.
2. Dalmau J, Tuzun E, Wu HY, et al. Paraneoplastic anti-N-methyl-D-aspartate receptor encephalitis associated with ovarian teratoma. *Ann Neurol.* 2007;61:25-36.
3. Titulaer MJ, McCracken L, Gabilondo I, et al. Treatment and prognostic factors for long-term outcome in patients with anti-NMDA receptor encephalitis: an observational cohort study. *Lancet Neurol.* 2013;12:157-165.
4. Dalmau J, Lancaster E, Martinez-Hernandez E, et al. Clinical experience and laboratory investigations in patients with anti-NMDAR encephalitis. *Lancet Neurol.* 2011;10:63-74.
5. Dalmau J. NMDA receptor encephalitis and other antibody-mediated disorders of the synapse: The 2016 Cotzias Lecture. *Neurology.* 2016;87:2471-2482.
6. Lancaster E, Dalmau J. Neuronal autoantigens--pathogenesis, associated disorders and antibody testing. *Nat Rev Neurol.* 2012;8:380-390.
7. Tabata E, Masuda M, Eriguchi M, et al. Immunopathological significance of ovarian teratoma in patients with anti-N-methyl-d-aspartate receptor encephalitis. *Eur Neurol.* 2014;71:42-48.
8. Makuch M, Wilson R, Al-Diwani A, et al. N-methyl-D-aspartate receptor antibody production from germinal center reactions: Therapeutic implications. *Ann Neurol.* 2018;83:553-561.
9. Clark RM, Lynch MP, Kolp R, et al. The N-methyl-D-aspartate receptor, a precursor to N-methyl-D-aspartate receptor encephalitis, is found in the squamous tissue of ovarian teratomas. *Int J Gynecol Pathol.* 2014;33:598-606.
10. Dabner M, McCluggage WG, Bundell C, et al. Ovarian teratoma associated with anti-N-methyl D-aspartate receptor encephalitis: a report of 5 cases documenting prominent intratumoral lymphoid infiltrates. *Int J Gynecol Pathol.* 2012;31:429-437.
11. Day GS, Laiq S, Tang-Wai DF, et al. Abnormal neurons in teratomas in NMDAR encephalitis. *JAMA Neurol.* 2014;71:717-724.
12. Tuzun E, Zhou L, Baehring JM, et al. Evidence for antibody-mediated pathogenesis in anti-NMDAR encephalitis associated with ovarian teratoma. *Acta Neuropathol.* 2009;118:737-743.

13. Cundiff CA, Elawabdeh N, Naguib MM, et al. Does MAP2 have a role in predicting the development of anti-NMDAR encephalitis associated with benign ovarian teratoma? A report of six new pediatric cases. *Pediatr Dev Pathol.* 2015;18:122-126.
14. Jandu AS, Odor PM, Vidgeon SD. Status epilepticus and anti-NMDA receptor encephalitis after resection of an ovarian teratoma. *J Intensive Care Soc.* 2016;17:346-352.
15. Scully RE. *Tumors of the Ovary and Maldeveloped Gonads. Second Series. Fascicle 16.* Washington, D.C.: Armed Forces Institute of Pathology; 1979.
16. Yanai-Inbar I, Scully RE. Relation of ovarian dermoid cysts and immature teratomas: an analysis of 350 cases of immature teratoma and 10 cases of dermoid cyst with microscopic foci of immature tissue. *Int J Gynecol Pathol.* 1987;6:203-212.
17. Arias C, Arrieta I, Massieu L, et al. Neuronal damage and MAP2 changes induced by the glutamate transport inhibitor dihydrokainate and by kainate in rat hippocampus in vivo. *Exp Brain Res.* 1997;116:467-476.
18. McPhail LT, McBride CB, McGraw J, et al. Axotomy abolishes NeuN expression in facial but not rubrospinal neurons. *Exp Neurol.* 2004;185:182-190.
19. Blumcke I, Becker AJ, Normann S, et al. Distinct expression pattern of microtubule-associated protein-2 in human oligodendrogliomas and glial precursor cells. *J Neuropathol Exp Neurol.* 2001;60:984-993.
20. He Y, Hong Y, Mizejewski GJ. Engineering alpha-fetoprotein-based gene vaccines to prevent and treat hepatocellular carcinoma: review and future prospects. *Immunotherapy.* 2014;6:725-736.
21. Gure AO, Stockert E, Scanlan MJ, et al. Serological identification of embryonic neural proteins as highly immunogenic tumor antigens in small cell lung cancer. *Proc Natl Acad Sci U S A.* 2000;97:4198-4203.
22. Kelly HA. *Ovariotomy* in Operative Gynecology. New York: D. Appleton and Company; 1909:307.
23. Willis RA. The structure of teratomata. *Journal of Pathology and Bacteriology.* 1935;40:1-36.
24. Willis RA. A further study of the structure of teratomata. *Journal of Pathology and Bacteriology.* 1937;45:49-65.

FIGURE LEGENDS

Figure 1

On initial gross examination, some NMDAR-E teratomas appeared normal (A) and did not contain obvious features of a teratoma (B), though simple cysts were present. A small nodule (B, arrow) corresponded to a Rokitansky nodule (C, arrow), within which neuroglial tissue (C, arrowhead) was surrounded by adipose and cutaneous teratomatous elements. Some NMDAR-E teratomas were mildly enlarged (D) and contained multiple follicle cysts (E), but no obvious features of a teratoma. A small nodule (E, arrows) corresponded to a Rokitansky nodule (F, arrow), within which was neuroglial tissue surrounded by adipose and cutaneous teratomatous elements.

Figure 2

Most NMDAR-E teratomas consisted of a 1 to 2 cm hair-bearing Rokitansky nodule within a cyst (A); the neuroglial tissue was located in the center (B, arrow) or in a subependymal distribution along cyst walls (B, arrowheads). In some cases, the Rokitansky nodule nearly obliterated the cyst cavity (C, D; arrow indicates neuroglial tissue) or entirely filled the cyst, resulting in a solid appearance (E, arrow; F, arrow). The adjacent cyst (E, arrowheads) was a mucinous cystadenoma (F, double arrowheads). The neuroglial tissue was in the center of the Rokitansky nodule (F, single arrowhead).

Figure 3

A minority of the NMDAR-E teratomas were cystic without a discrete Rokitansky nodule; one case exhibited typical features of matted hair, sebaceous material, fat and cartilage (A). The mediastinal NMDAR-E teratoma was predominantly solid and fleshy with focal cystic features (B).

Figure 4

Neuropil-associated neuroglial tissue (A, arrow) was present in the center of the Rokitansky nodule in each of the NMDAR-E teratomas and was surrounded by a variable number of lymphoid aggregates containing germinal centers ranging from numerous confluent aggregates

to just a few (B to F). Lymphoid aggregates with germinal centers surrounding neuropil were more frequent in NMDAR-E teratomas compared to control teratomas (G). In contrast, lymphoid aggregates that lack germinal centers were present adjacent to neuropil to the same extent in both groups of teratomas (H). Each tumor is represented with a symbol; solid lines indicate the median and 95% confidence interval (****, $p<0.001$; ns, not significant).

Figure 5

In some cases of NMDAR-E teratoma, neuroglial tissue was located beneath a layer of ependyma lining the wall of a cyst (so-called glial cyst) (A to F). The cyst was located either within (A) or adjacent (B) to the Rokitansky nodule. Choroid plexus was often present (E). Lymphoid aggregates with germinal centers were present (E, F).

Figure 6

Mature neurons were rare and showed degenerative features within neuropil in NMDAR-E teratomas (A, B) compared to control teratomas (C,D). Degenerative features included shrunken neuronal nuclei with smudged contours and cytoplasmic vacuolation (A, black arrowhead), and chromatolysis (A, blue arrowhead; B, black arrowhead). The cellularity of mature neurons within the CNS-like neuropil was significantly lower in NMDAR-E teratomas (E). Each tumor is represented with a symbol; solid lines indicate the median and 95% confidence interval (***; $p<0.001$). Scale bars, 50 μm.

Figure 7

Immunostaining for neural markers highlights differences in neural cell populations in NMDAR-E teratomas versus control teratomas. NeuN positive mature neurons were rare in NMDAR-E teratomas (A) compared to control teratomas (D); the difference was statistically significant (G). MAP2+ small cells with blunted process were frequent in NMDAR-E teratoma (B). The cellularity of MAP2+ cells in control teratomas (E) was the same (H) but these cells had normal dendritic processes rather than blunted processes. The cellularity of OLIG2+ oligodendrocytes in NMDAR-E teratomas (C) and in control teratomas (F) was similar (I). In G-I, each evaluated tumor is represented with a symbol; solid lines indicate the median and 95% confidence interval (**, $p<0.01$; ns, not significant). Scale bars, 50 μm.

Figure 8

Astrocytes were hypercellular in NMDAR-E teratomas (A-C) compared to control teratomas (D-F) and exhibited unusual dysmorphic features such as hyperchromasia and mild pleomorphism (A), multinucleation (B), or abundant eosinophilic deposits (C). Such features were not present in control teratomas, although some exhibited Rosenthal fibers (E) or gemistocytic features (F). The cellularity of astrocytes was significantly higher in NMDAR-E teratomas (G). Each tumor is represented with a symbol; solid lines indicate the median and 95% confidence interval (****; $p<0.0001$). Scale bars, 50 μm.

Figure 9

Ganglion cell clusters were equally present in NMDAR-E teratomas (A, B) and in control teratomas (C, D). While scattered lymphocytes were present in and around ganglion cell clusters in both groups of teratomas, lymphoid aggregates with germinal centers were present in a subset of NMDAR-E teratomas (A) but not in any of the control teratomas (C). There was no difference in the number of ganglion cell clusters between the two groups of teratomas (E). Ganglion cell cluster-associated lymphoid aggregates were equally present in NMDAR-E teratomas as in control teratomas, regardless of whether germinal centers were present (F, G). Each tumor is represented with a symbol; solid lines indicate the median and 95% confidence interval (ns, not significant). Scale bars, 50 μm.

Supplementary Figure S1.

Neuroglial tissue was more abundant in the NMDAR-E teratomas compared to control teratomas. Each tumor is represented with a symbol; solid lines indicate the median and 95% confidence interval. (**, $p<0.01$)

Supplementary Figure S2.

Lymphoplasmacytic infiltration of neuroglial tissue. A-C) Inflamed neuroglial tissue from a representative encephalitis-associated teratoma; H&E stain (A), T-cell marker CD3 (B), regulatory T-cell marker FOXP3 (C), B-cell marker CD20 (D), and plasma cell marker CD138 (E). F-J) Inflamed neuroglial tissue from a representative control teratoma; H&E stain (F), T-cell marker CD3 (G), regulatory T-cell marker FOXP3 (H), B-cell marker CD20 (I), and plasma cell marker CD138 (J). K) The maximum density of lymphocytes is slightly increased in NMDAR-E teratomas compared to control cases; however, the density of CD3-positive T-cells (L), FOXP3-positive regulatory T-cells (M), CD20-positive B-cells (N), and CD138-positive plasma cells (O) did not significantly differ between the two groups. Each evaluated tumor is represented with a symbol; solid lines indicate the median and 95% confidence interval (K, O) or the group mean and SEM (L-N). (**, $p<0.01$; ns, not significant) Scale bars, 50 μm.

Supplementary Figure S3.

Lymphoid aggregates in non-neural tissues. A-B) Representative images of lymphoid aggregates with and without germinal centers adjacent to non-neural tissues including adnexal structures and mucinous epithelium in NMDAR-E teratomas. C-D) Representative images of lymphoid aggregates with and without germinal centers adjacent to non-neural tissues in control teratomas. E) The number of germinal centers involving non-neural tissues is similar between the two groups. F) The number of lymphoid aggregates without germinal centers is slightly higher in the control group, likely secondary to the larger tumor size. Each evaluated tumor is represented with a symbol; solid lines indicate the median and 95% confidence interval. (**, $p<0.01$; ns, not significant) Scale bars, 50 μm.

Supplementary Figure S4.

The follicles, oocytes, and ovarian stroma (A to C) appeared normal in the NMDAR-E teratomas, without any lymphocyte infiltrate or lymphoid aggregates. Most of these women also had multiple follicle cysts (D).

Tables

Table 1

	NMDAR-E Teratomas	Control Teratomas	p-value
Overall tumor size	1.9 cm	7.5 cm	<0.0001
Neuroglial Population			
Total surface area of neuroglial tissues	0.1 cm^2	0.5 cm^2	<0.001
Percent of teratoma composed of neuroglial tissues	5.2%	1.3%	<0.01
Mature neurons per hpf of neuropil	1	7	<0.001
Astrocytes per hpf of neuropil	200	97	<0.0001
Presence of ganglion cell clusters	5/12 (42%) tumors	10/61 (16%) tumors	NS
Ganglion cell clusters per tumor	0	0	NS
NeuN positive cells per hpf of neuropil	0	18	<0.01
MAP2 positive cells per hpf of neuropil	19	20	NS
OLIG2 positive cells per hpf of neuropil	17 ± 3*	24 ± 9*	NS
Immune Cell Population involving Neuroglial Tissue			
Presence of diffuse lymphoplasmacytic infiltrates in neuropil	4/12 (33%) tumors	26/61 (43%) tumors	NS
Diffuse lymphoplasmacytic infiltrate in neuropil (cells/hpf)	30	14	<0.05
Presence of lymphoid aggregates without germinal centers around neuropil	12/12 (100%) tumors	43/61 (70%) tumors	<0.05
Presence of lymphoid aggregates without			

germinal centers around ganglion cell clusters	4/5 (80%) tumors	1/9 (11%) tumors	<0.05
Lymphoid aggregates without germinal centers around neuropil (number per tumor)	3	1	NS
Lymphoid aggregates without germinal centers around ganglion cell clusters (number per tumor)	2	0	NS
Presence of lymphoid aggregates with germinal centers around neuropil	11/12 (92%) tumors	4/61 (7%) tumors	<0.0001
Presence of lymphoid aggregates with germinal centers around ganglion cell clusters	2/5 (40%) tumors	0/9 (0%) tumors	NS
Lymphoid aggregates with germinal centers around neuropil (number per tumor)	3	0	<0.0001
Lymphoid aggregates with germinal centers around ganglion cell clusters (number per tumor)	0	0	NS
CD20 positive cells per hpf of neuropil	3 ± 1*	3 ± 1*	NS
CD138 positive cells per hpf of neuropil	7	12	NS
CD3 positive cells per hpf of neuropil	28 ± 8*	23 ± 5*	NS
FOXP3 positive cells per hpf of neuropil	8 ±3*	6 ± 2*	NS
Ratio of CD3 to FOXP3 positive cells	0.38 ± 0.91*	0.25 ± 0.09*	NS
Immune Cell Population involving Non-Neuroglial Tissue			
Presence of diffuse lymphoplasmacytic infiltrates	1/12 (8%) tumors	11/61 (18%) tumors	NS
Presence of lymphoid aggregates without germinal centers	11/12 (92%) tumors	61/61 (100%) tumors	NS

Lymphoid aggregates without germinal centers (number per tumor)	3	10	<0.01
Presence of lymphoid aggregates with germinal centers	5/12 (42%) tumors	15/61 (25%) tumors	NS
Lymphoid aggregates with germinal centers (number per tumor)	0	0	NS

Legend:
All values represent the median unless indicated by an *, which designates values reported as statistical mean ± standard error of the mean
NS: not significant ($p>0.05$)
hpf: high power field (400X magnification)

Table 2 Histopathologic Studies of NMDAR Teratomas

Study	NMDAR-E Teratomas (n)	Control Teratomas (n)	Lymphoid Aggregates with Germinal Centers in Neuroglial Tissue (NMDAR-E versus control)	Major Neuroglial Tissue Findings
Current study	12	61	11/12 versus 4/61	Relative absence of mature neurons in NMDAR
Dalmau et al., 2007	12	0	not studied	NR2 detected on neuroglial tissue. MAP2 positive immature neurons present.
Tuzun et al., 2009	9	3	not studied	NR1, NR2 detected on neuroglial tissues. B-lymphocyte infiltrates more extensive in NMDAR teratomas
Cundiff et al. 2015	6	6	not studied	NeuN and MAP2 positive cell populations similar in NMDAR and control teratomas
Dabner et al., 2012	5	22	3/5 versus 0/22	Degenerative changes in 2/5 NMDAR versus 0/22 control teratomas
Day et al., 2014	4	20	not studied	Lymphoid infiltrates around neuroglial tissue in 4/4 NMDAR teratomas versus 0/20 sporadic teratomas. "Dysplastic" neurons in 4/4 NMDAR teratomas versus 0/20 control teratomas.
Clark et al., 2014	5	10	not studied	NR1, NR2 detected by immunostains in neuroglial tissue and in squamous epithelium of both NDMAR teratomas and control teratomas
Tabata et al., 2014	3	23	not studied	Increased B-cell population around neuroglial tissue in NMDAR teratomas; NR1 NR2 detected by immunostains
Makuchet al., 2018	2	0	not studied	Antibodies to NR1, NR2 detected in germinal center of lymphoid aggregates

Figure 1

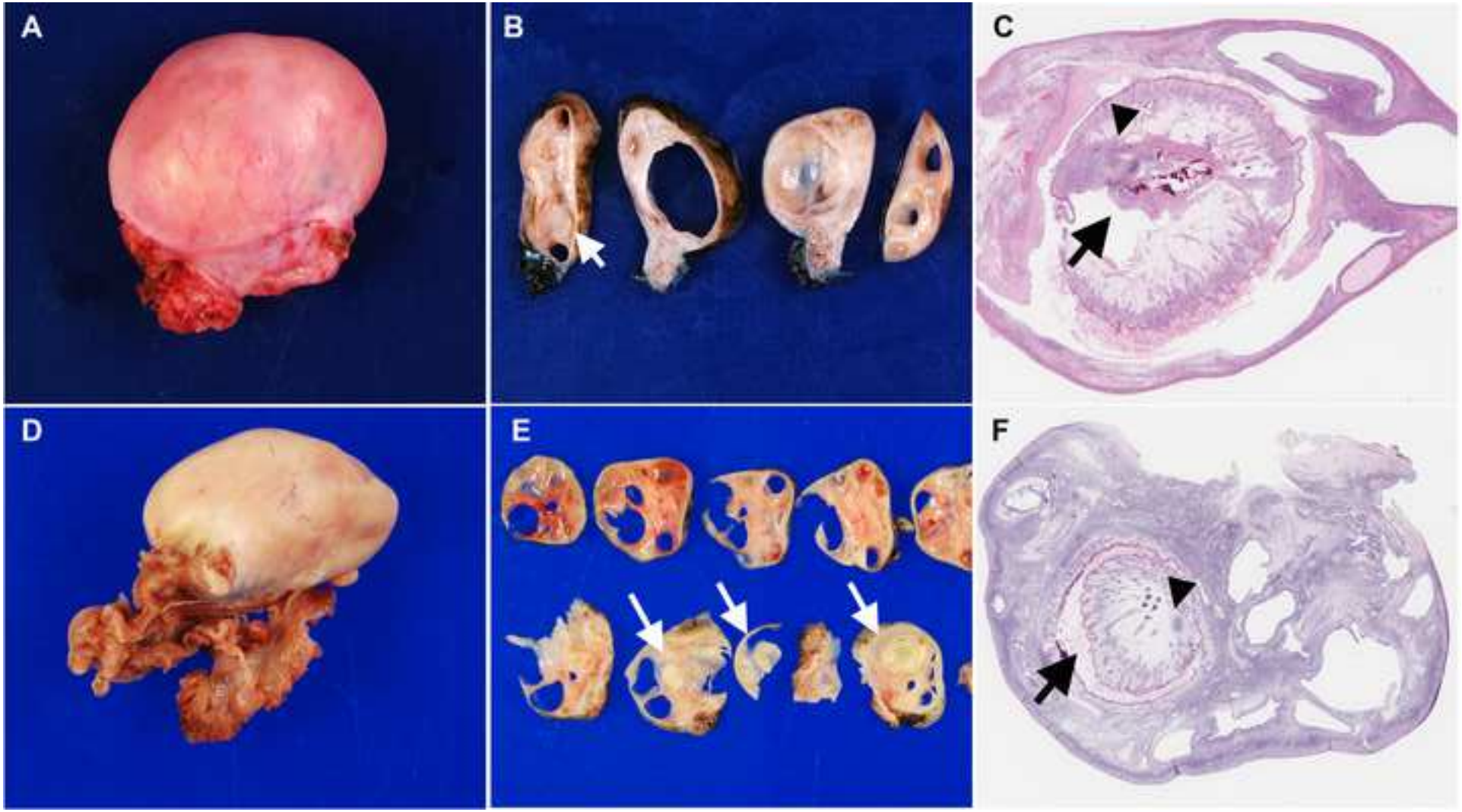

Figure 2

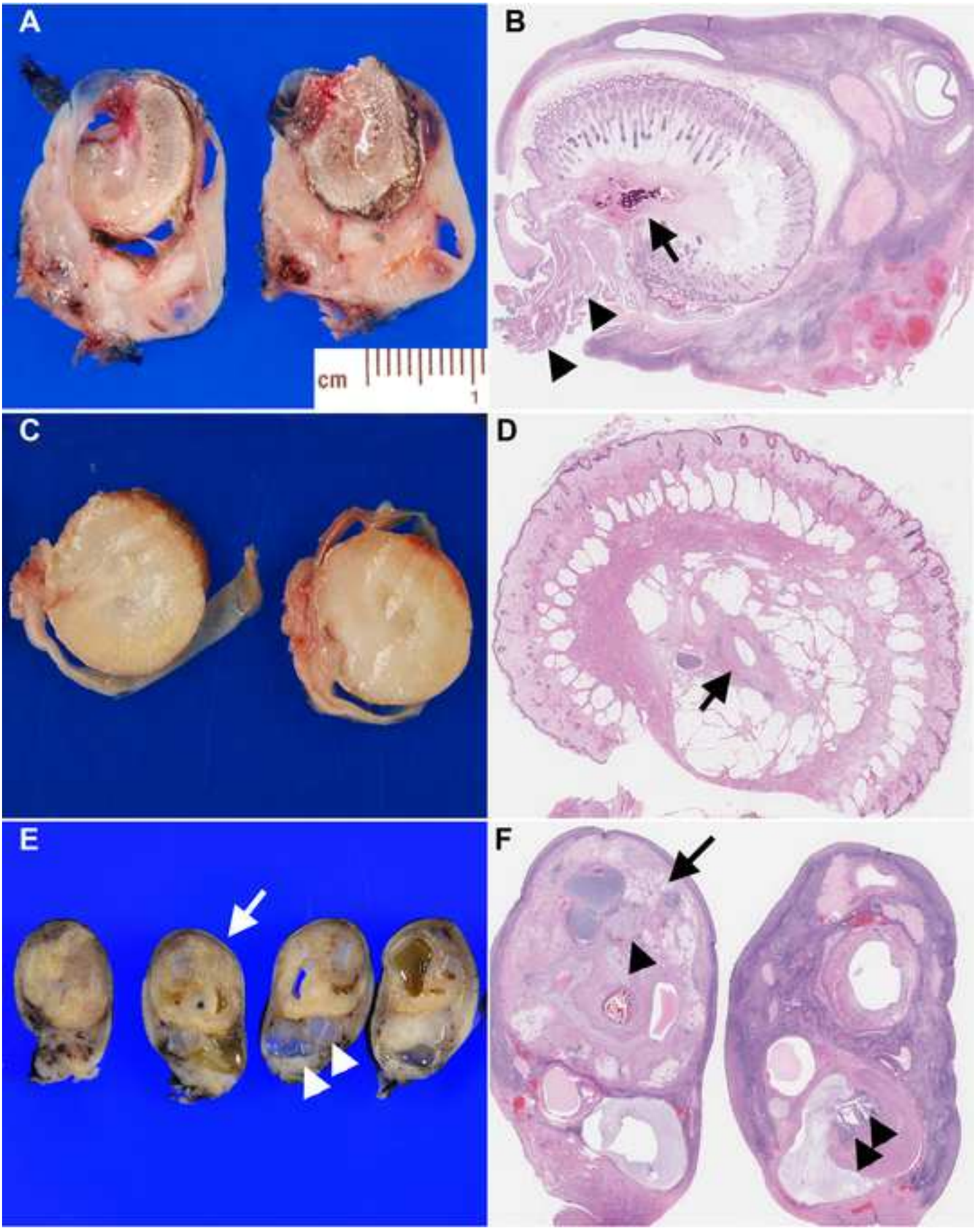

Figure 3

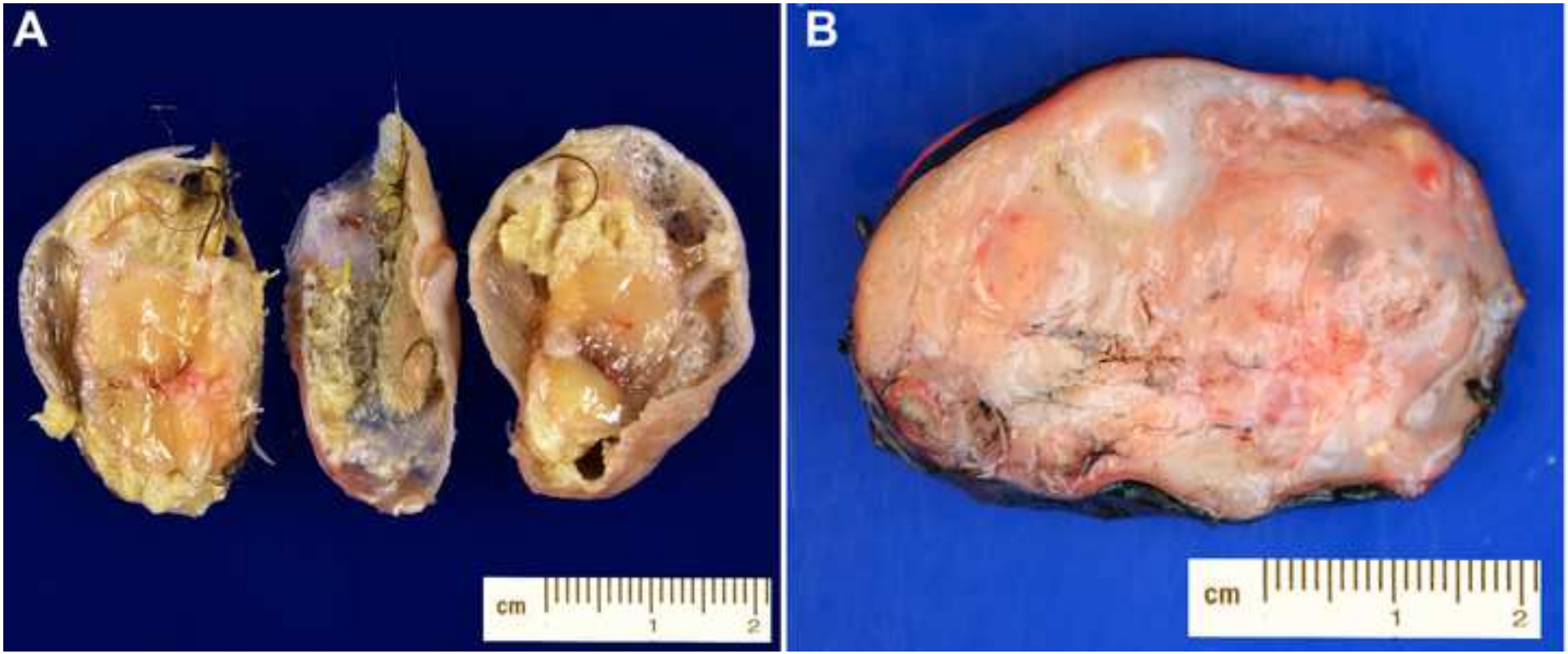

Figure 4 revised

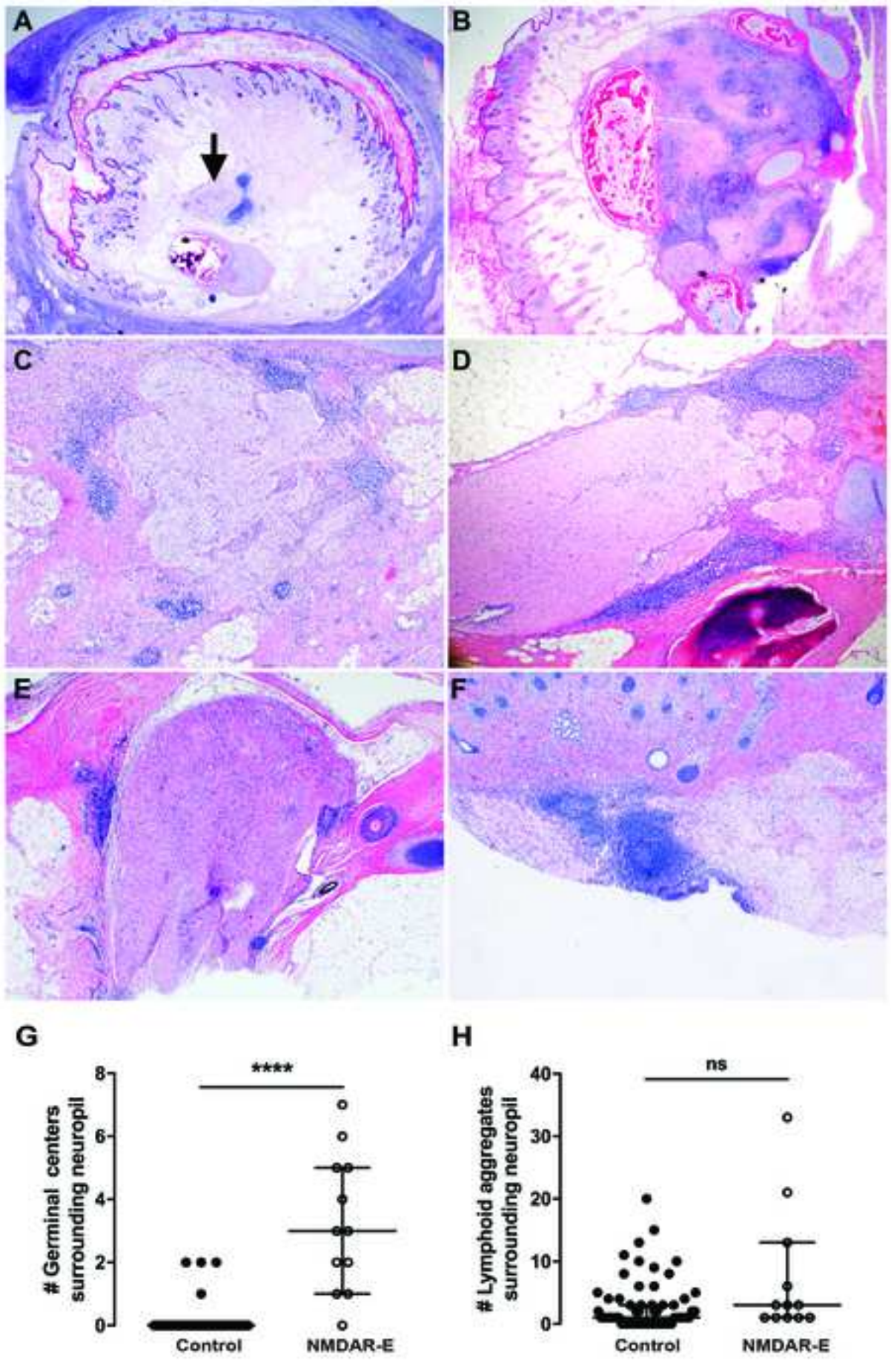

Figure 5

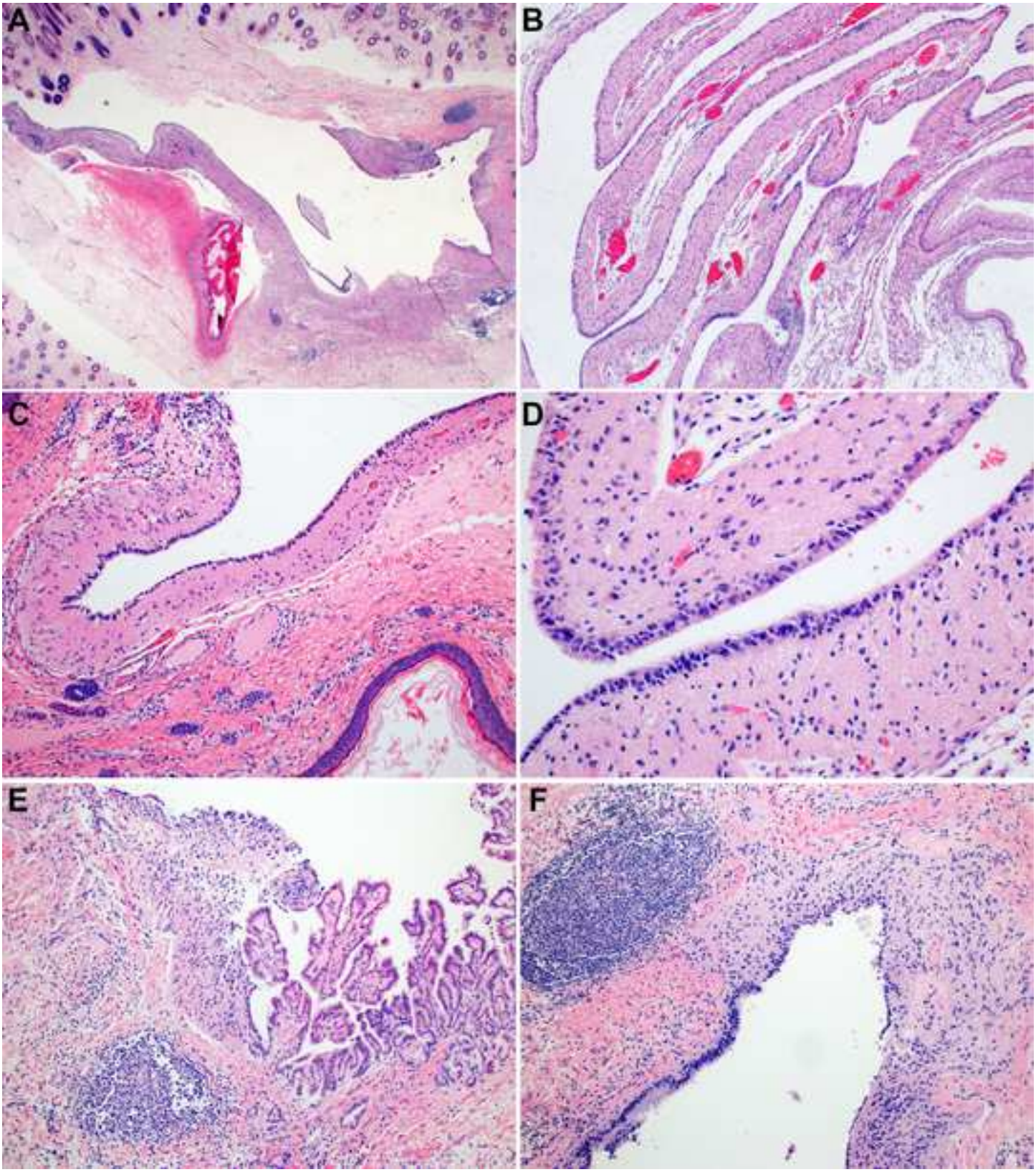

Figure 6 revised

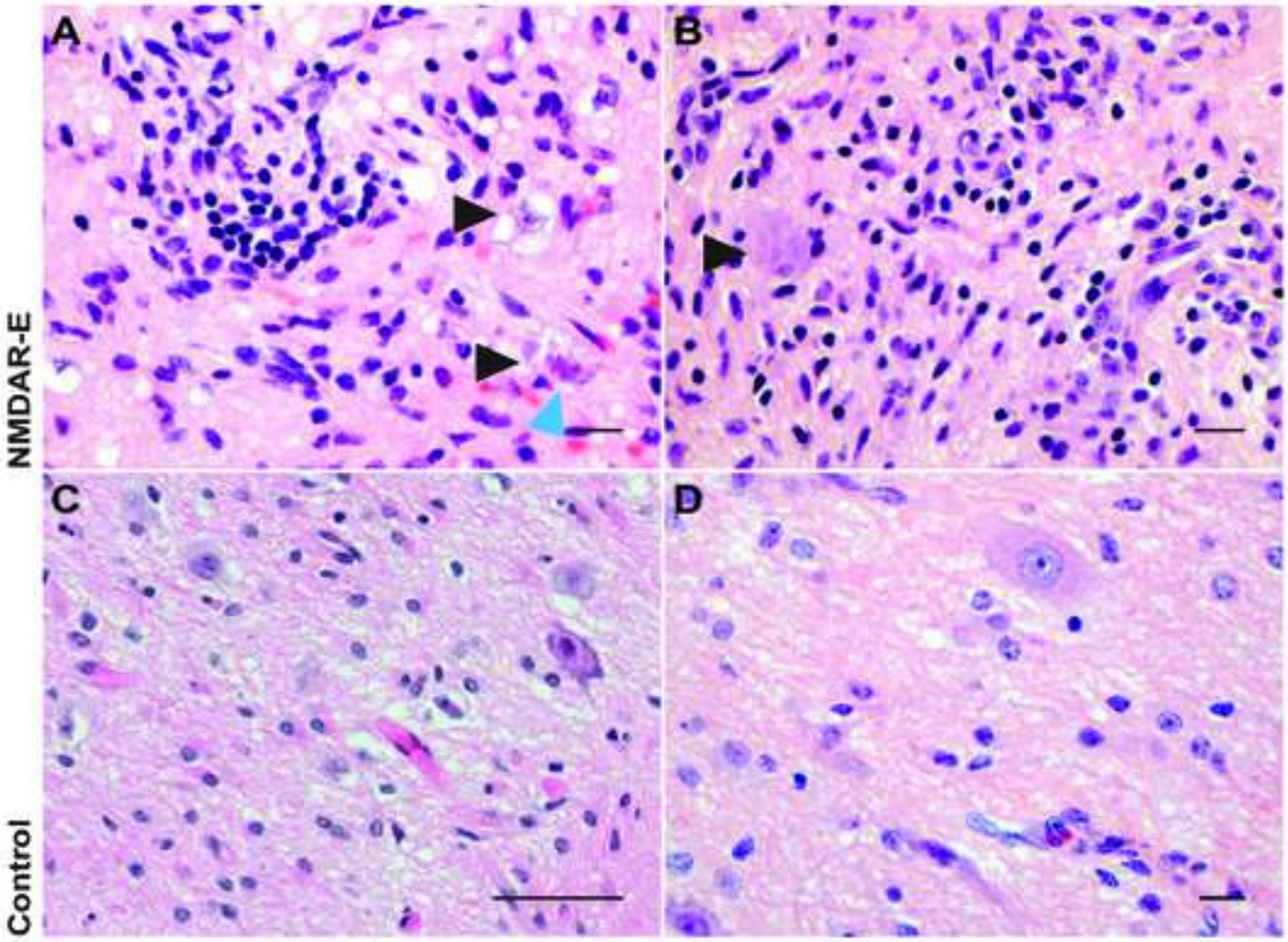

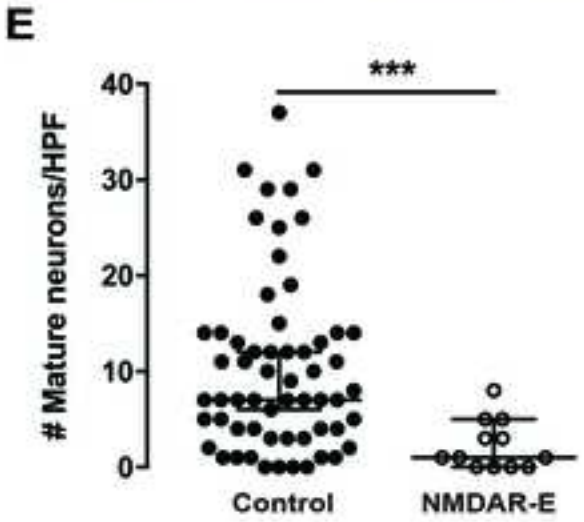

Figure 7

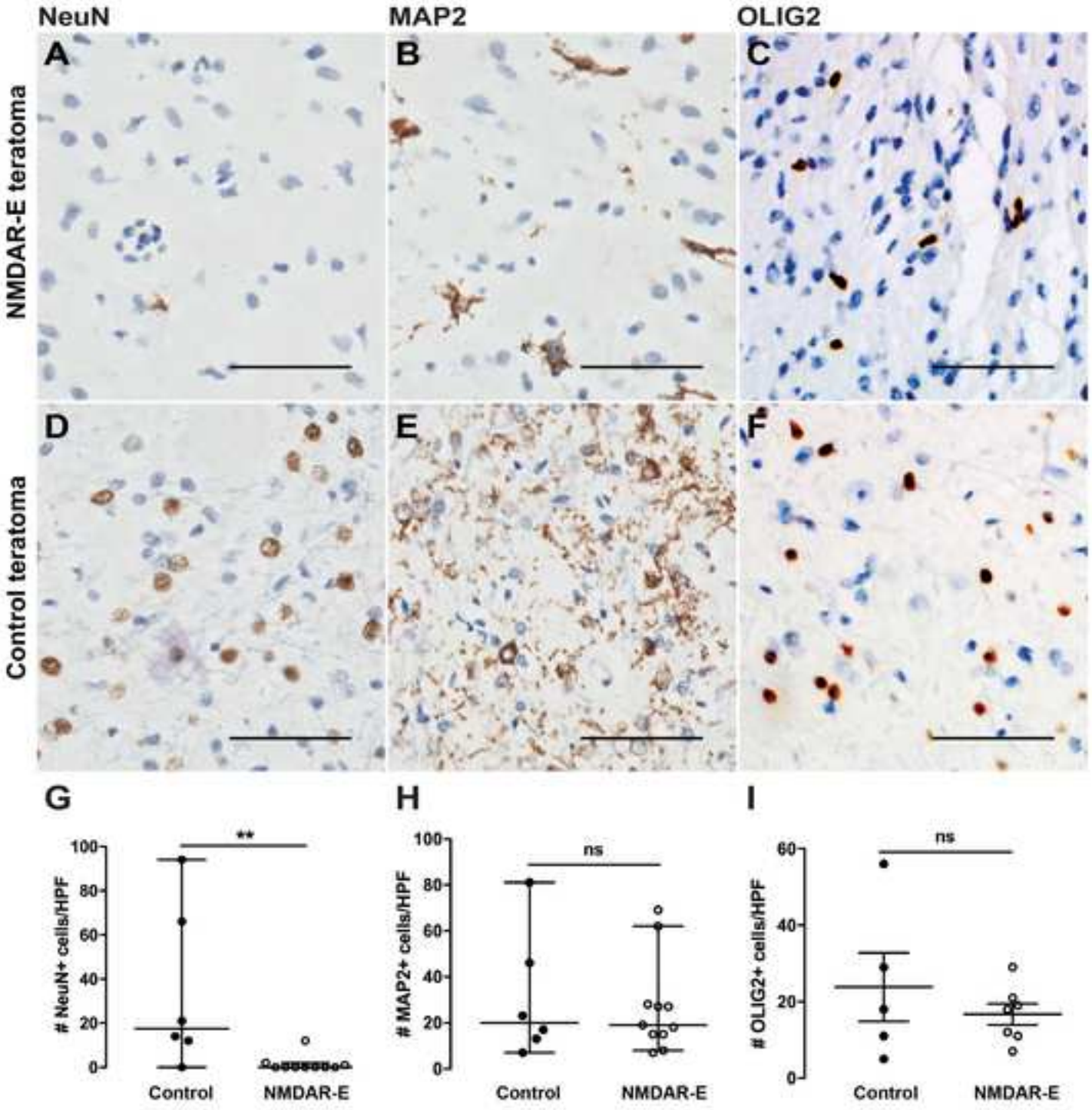
NeuN
MAP2
OLIG2
A
B
C
D
E
F
NMDAR-E teratoma
Control teratoma
G
H
I
NeuN+ cells/HPF
MAP2+ cells/HPF
OLIG2+ cells/HPF
**
ns
ns
Control
NMDAR-E
Control
NMDAR-E
Control
NMDAR-E

Figure 8 revised

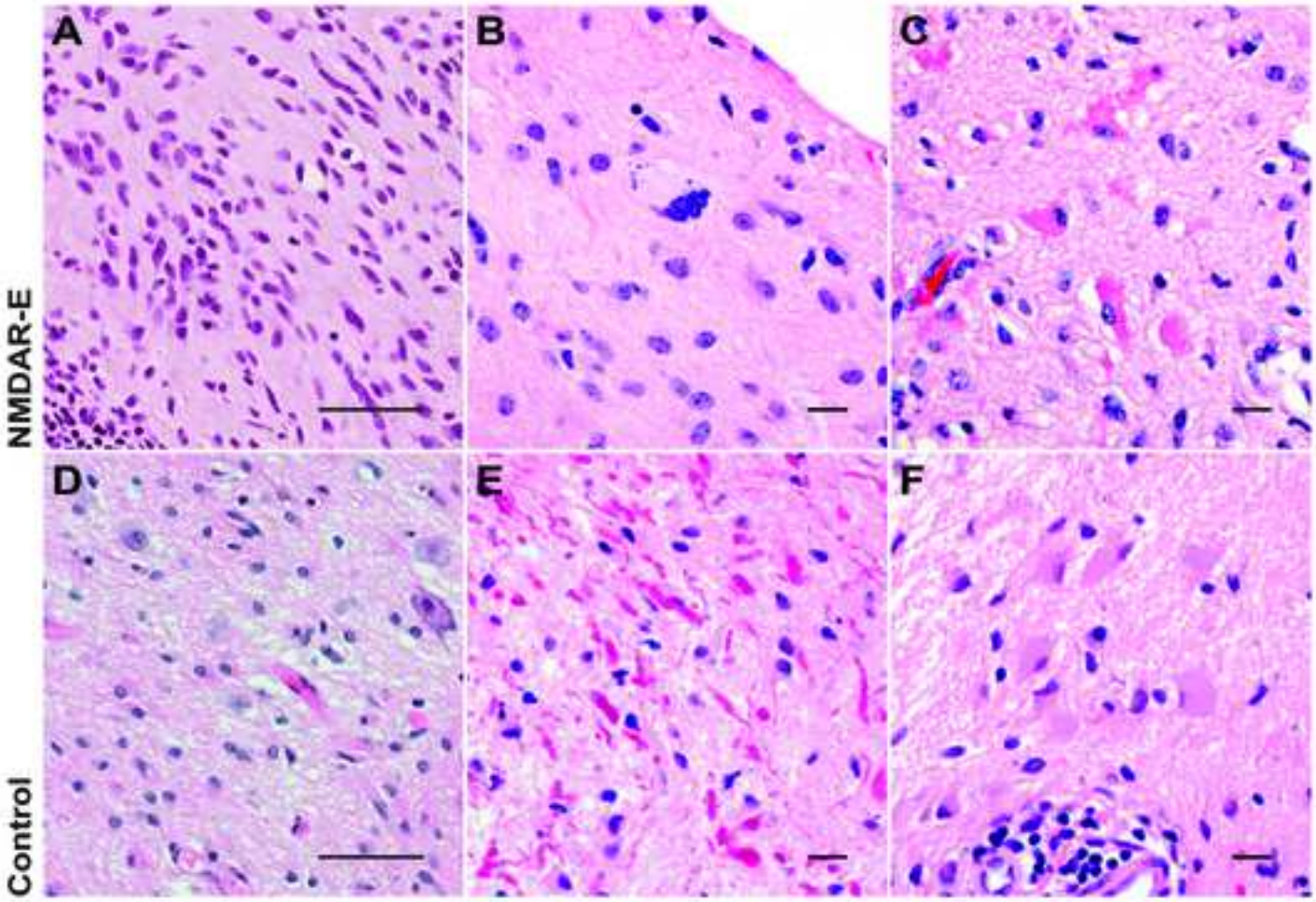

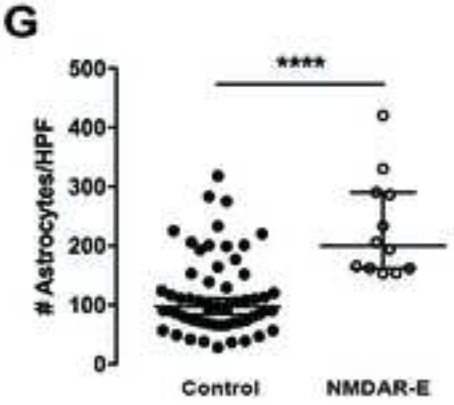

Figure 9 revised

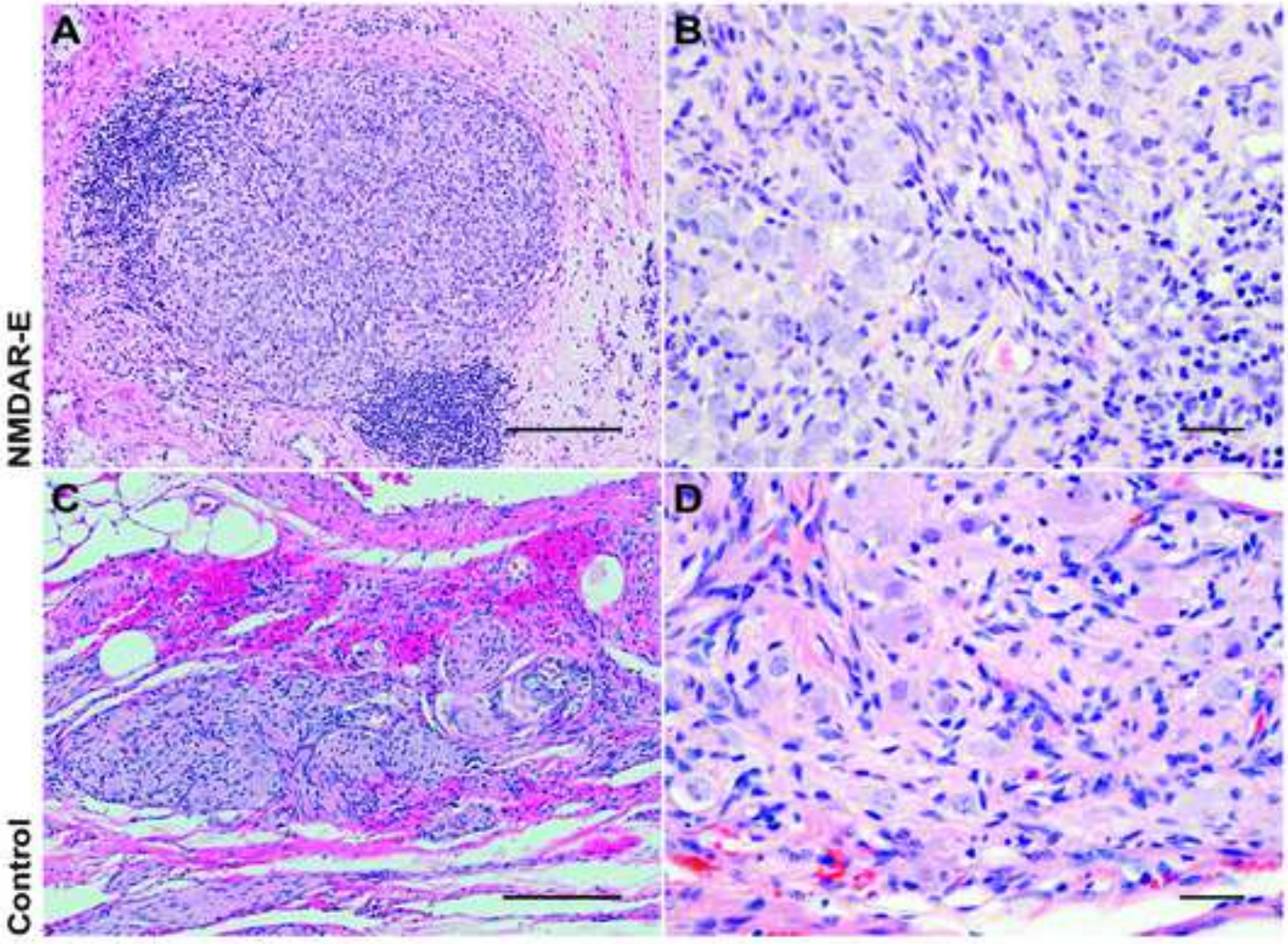

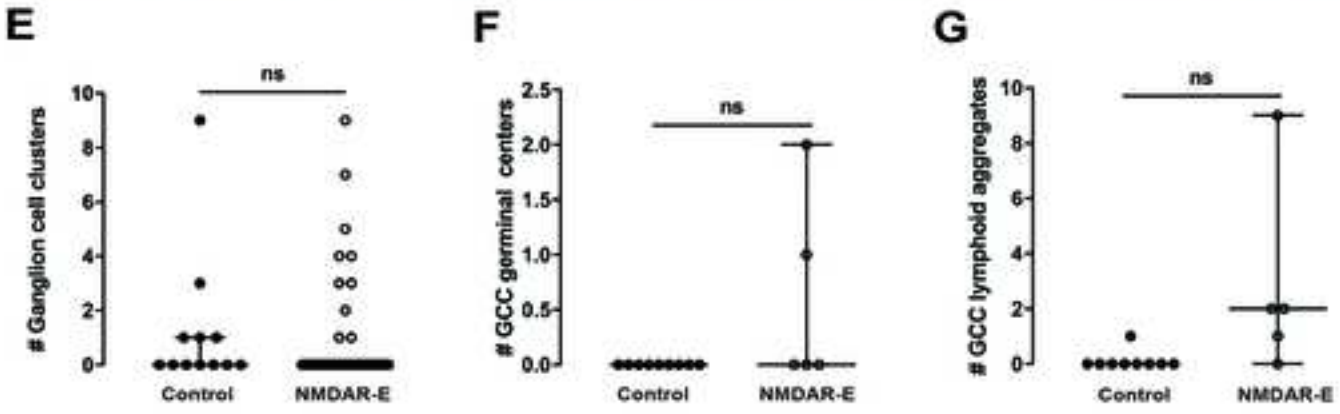

Figure S1

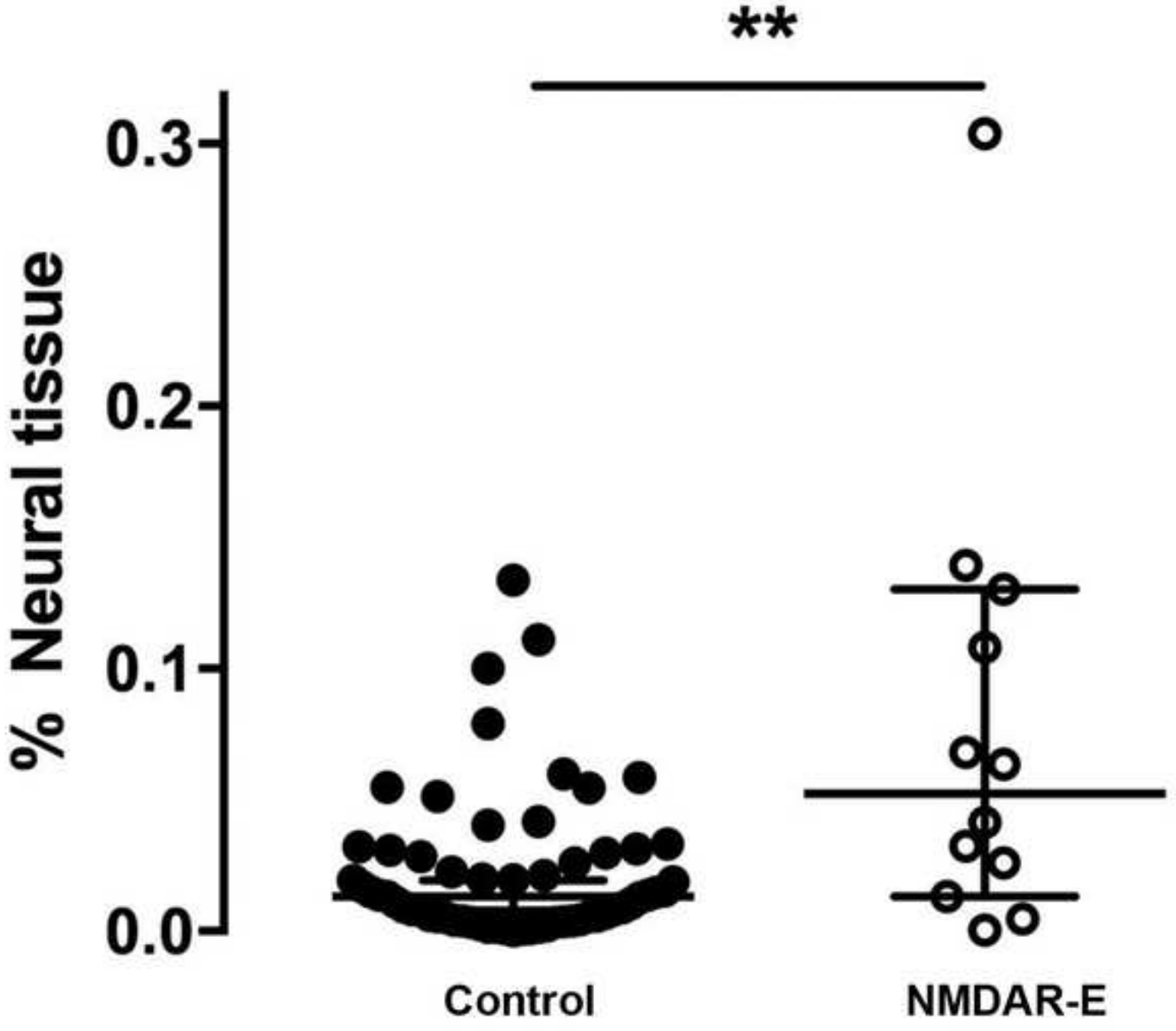

Figure S2

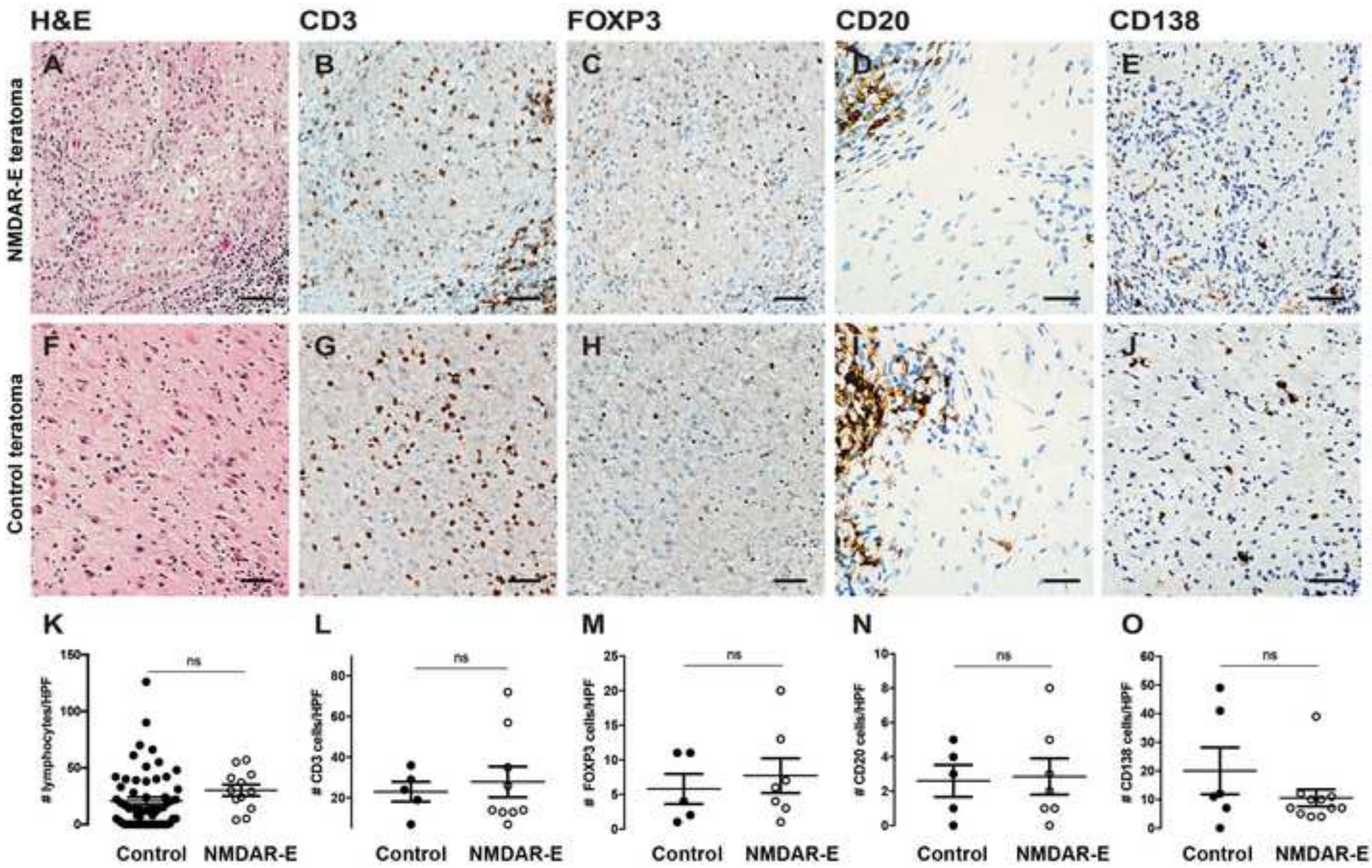
H&E
CD3
FOXP3
CD20
CD138
NMDAR-E teratoma
Control teratoma
A
B
C
D
E
F
G
H
I
J
K
L
M
N
O
lymphocytes/HPF
CD3 cells/HPF
FOXP3 cells/HPF
CD20 cells/HPF
CD138 cells/HPF
ns
Control
NMDAR-E

Figure S3

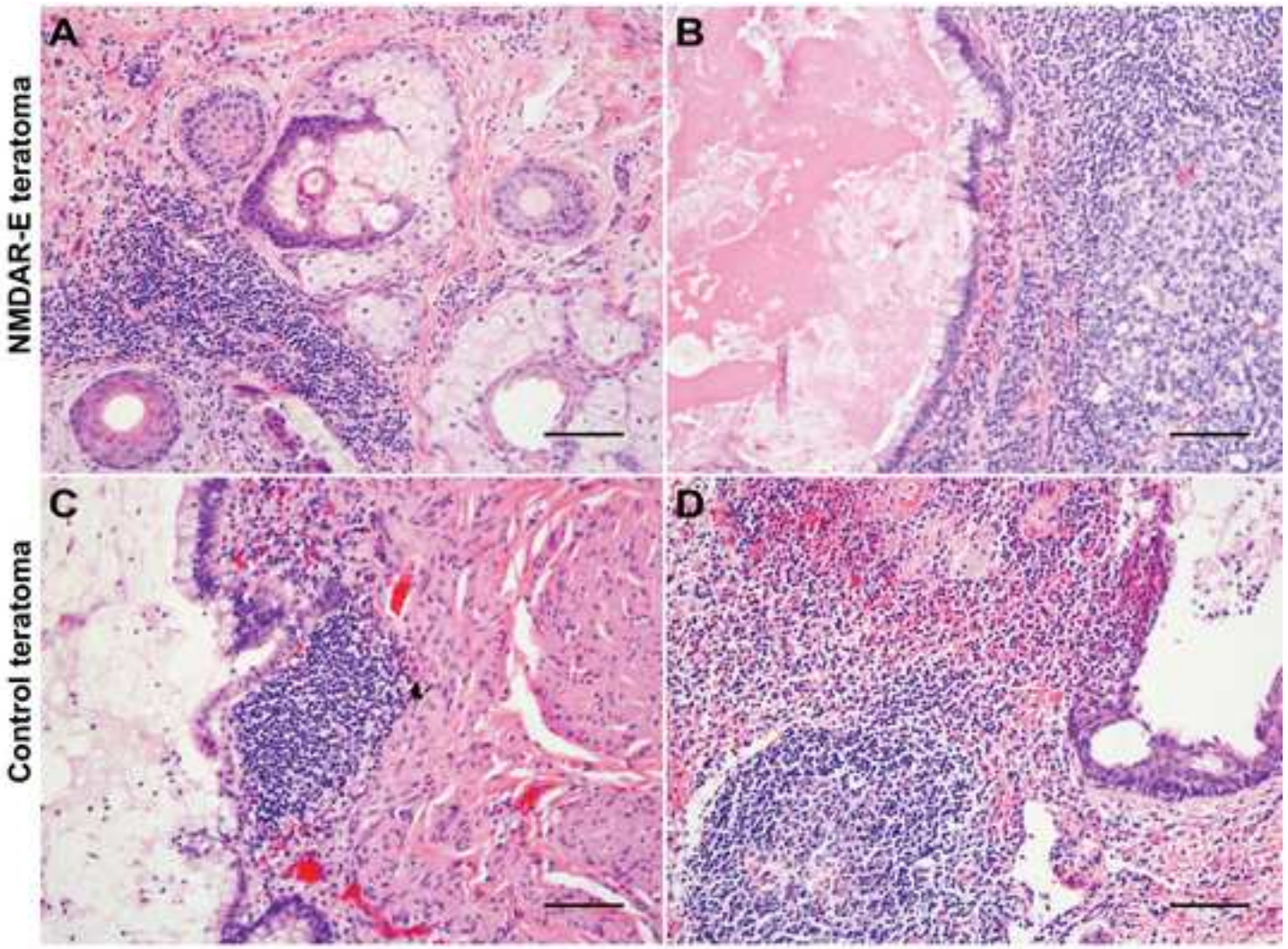
A
B
C
D
NMDAR-E teratoma
Control teratoma

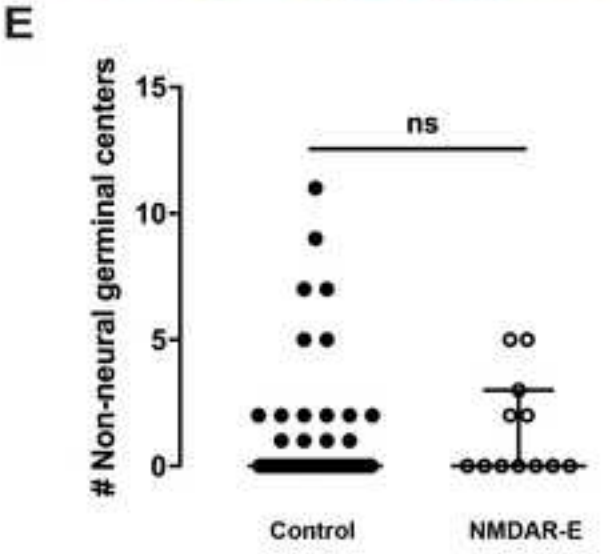
E
Non-neural germinal centers
15
10
5
0
ns
Control
NMDAR-E

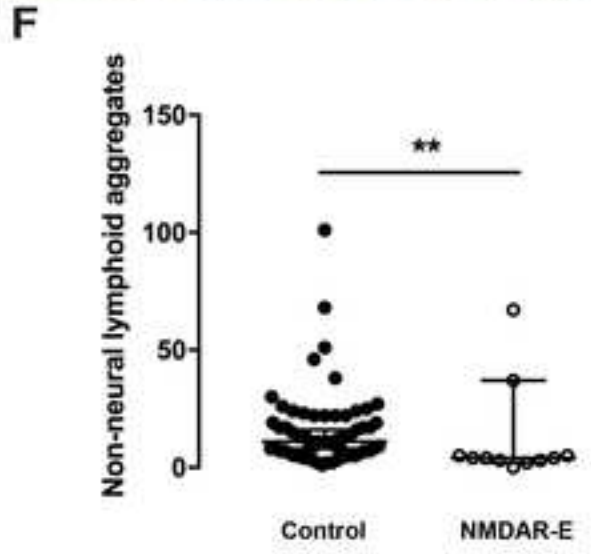
F
Non-neural lymphoid aggregates
150
100
50
0
**
Control
NMDAR-E

Figure S4